International Astronautical Congress, Milan, Italy, 14-18 October 2024.

IAC-24,A6,IP,12,x88750

Initial Pose Acquisition Phase for Active Debris Removal Missions

Bronislovas Razgus[a]*, **Michele Maestrini**[b], **Pierluigi Di Lizia**[c]

[a] *PhD candidate, Antanas Gustaitis Aviation Institute, Vilniustech, Vilnius, Lithuania* E-mail: bronislovas.razgus@vilniustech.lt

[b] *Assistant Professor, Department of Aerospace Science and Technology, Politecnico di Milano, Milan, Italy* E-mail: michele.maestrini@polimi.it

[c] *Associate Professor, Department of Aerospace Science and Technology, Politecnico di Milano, Milan, Italy* E-mail: pierluigi.dilizia@polimi.it

* Corresponding author

Abstract

Space debris is one of the biggest challenges in space exploration. Without any actions, a situation called a Kessler syndrome might occur, which would forbid humankind's access to space. To avoid this situation, the generation of new debris needs to be reduced to a minimum, which means that we have to actively remove old, uncooperative space objects from the orbits they occupy. This requires a dedicated mission to rendezvous with the object, capture, and de-orbit it. Navigating near the satellite presents a serious challenge for the Guidance, Navigation, and Control (GNC) system, especially when a priori information on the state of the object is not known. The system has to be initialised with a pose that the tracking algorithms could then use to perform the mission. In this paper, the initial pose acquisition phase is analyzed, in particular using a previously developed Perspective Principal Line (PPL) method. This method employs a specific version of the Perspective-n-Line (PnL) methods, where the pose is estimated from the projected and 3D line correspondence. In the PPL case, these lines are the principal (reference frame) axes. It is a computationally inexpensive algorithm that can run on a dedicated hardware in real-time and deliver sufficient accuracy, however, it requires certain conditions to be met. This paper addresses the constraints that this algorithm puts on the mission, e.g. initial distance, illumination conditions, and certain properties of the target satellite. Furthermore, the design of this phase is presented and it is shown that if an appropriate scenario is chosen, the PPL method could be a reliable tool for initial pose acquisition.

1. Introduction

One of the main challenges in Active Debris Removal (ADR) missions is for the Guidance, Navigation, and Control (GNC) system. The key challenge is estimating the relative pose of the target object without prior information. Various techniques, including active sensors such as LIDARs [1, 2] and passive ones like cameras [3–5], have been proposed. From a cost point of view, LIDARs are often excluded due to their relatively high cost compared to cameras. Thermal infrared imaging is also proposed [6, 7] to avoid eclipse conditions, however, the most common approach is to use visual spectra cameras, due to ease of operation and cost. Vision-based pose estimation relies on extracting features (points, lines) from an image and matching them with the corresponding features in a 3D model. After acquiring the initial pose, it can be tracked and refined using PnP/PnL methods, combined with least squares, RANSAC, ICP, and similar algorithms. [8]. However, the initial pose acquisition is the challenging part, because these correspondences are not present. There are mainly two approaches to this problem: model-based and Neural Network (NN) based [9]. The latter processes the image and outputs either the pose directly or provides feature correspondences, which are then fed into one of the solvers. In fact, neural network-based methods solve the correspondence problem at every step. The downside of NN methods is the relatively high computational load, which usually requires dedicated graphic processing units. Model-based solutions are based on generating candidate solutions, which are then evaluated with reprojection errors. Our proposed solution [10] is based on lines as features and is detailed in the next section. It was shown that

if an object exhibits a rectangular shape, it is possible to estimate its principal lines (projected reference frame axes). Once these are known, there exists a set of candidate solutions for the attitude, which are then checked against the reprojections and the candidate is selected. In this paper, thus, the conditions for this algorithm to work are analyzed, which nevertheless are applicable for different methods as well. Different illumination conditions and approach scenarios are checked, and some guidelines for an initial pose acquisition phase are detailed.

2. Perspective Principal Lines method

Perspective Principal Lines (PPL) method aims to solve the initial pose acquisition problem by detecting lines as features and extracting the principal (reference frame) direction in the image [10]. Principal lines are estimated through a line-histogram method, where it is checked how many lines there are with given slope angles. The most prominent directions above a certain threshold are selected as candidate directions as in Fig. 1.

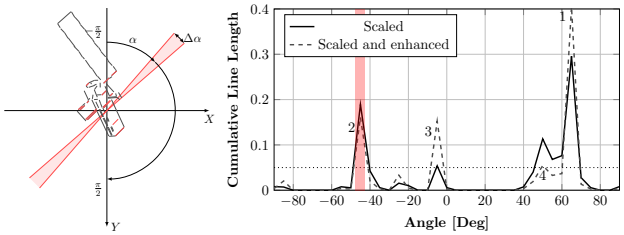

Fig. 1: Line histogram method to estimate prominent directions in the detected lines

For every set of candidate directions, there are eight possible solutions [10]. In addition to that, each three directions give six possible combinations for the x, y, and z directions, which totals to 48 candidates per three line set. If there are more prominent directions, this number increases even further. The solutions are then evaluated through reprojections and the one that matches most of the lines is selected as the estimate. The success of the PPL method strongly depends on the number of detected lines, which facilitates the estimation of the principal directions. This threshold has been found to be ≈ 50. The number of detections (on average) depends on the illumination conditions, which are discussed hereafter.

3. Illumination conditions

The line detector in question is a Line Segment Detector (LSD) [11]. Although the following analysis is specific to this detector, similar results are expected for different features and/or detectors. The solar angles α and β are defined relative to the camera frame C, and they act as elevation and azimuth angles when the camera is directed toward the target, Fig. 2.

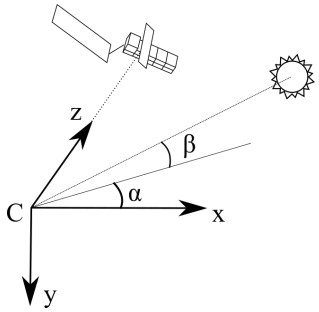

Fig. 2: Sun angles definition

Next, we will vary these angles in all possible directions to check how many lines on average are detected for a given sun direction. For this analysis, we chose Envisat as the target. One hundred images with random attitude were generated for each illumination condition and the average number of lines detected was recorded, Fig. 3.

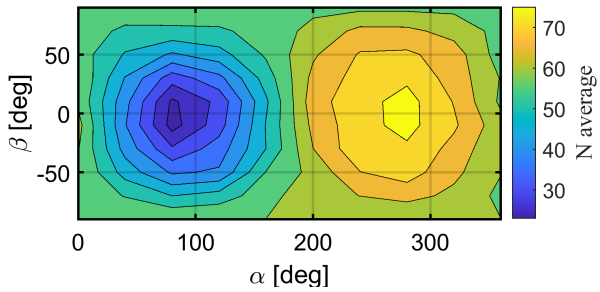

Fig. 3: Average number of lines detected for different Sun angles

The worst conditions happen when the Sun direction is coinciding with the target's direction ($\alpha = 90°$, $\beta = 0°$), since the shadow is cast and no light reaches the sensor. Optimal conditions occur when the sun vector aligns with the camera's boresight, minimizing shadows and maximizing line detection One can notice a symmetrical pattern in the distribution and, in fact, it is only the angle between the object's direction and the direction of Sun that matters, thus the plot can be condensed to a one-dimensional dependency as in Fig. 4. We can see that the sun angle has

to be more than $\approx 60°$ and larger for the 50-lines threshold to be satisfied on average.

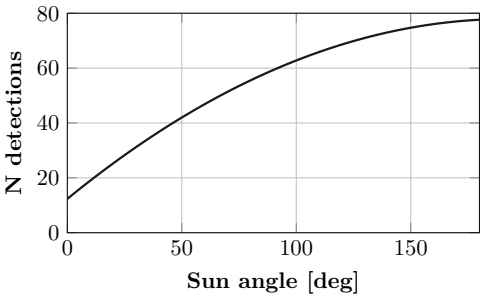

Fig. 4: Average number of lines detected

4. Target approach direction

To evaluate the illumination conditions, we first have to look at the eclipse conditions. Since an ADR mission would likely employ a camera in visible range, such a mission has to happen during the sunlight part of the orbit. see Fig. 5.

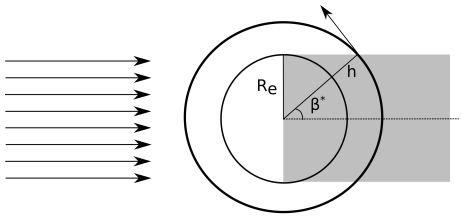

Fig. 5: Eclipse conditions

We define the critical angle for the eclipse, β^*, as [12]:

$$\beta^* = \sin^{-1} \frac{R_e}{R_e + h} \tag{1}$$

where R_e and h are the radius of Earth and orbital altitude respectively. The fraction of an orbit in illumination is then:

$$f = 1 - \frac{\beta^*}{\pi} \tag{2}$$

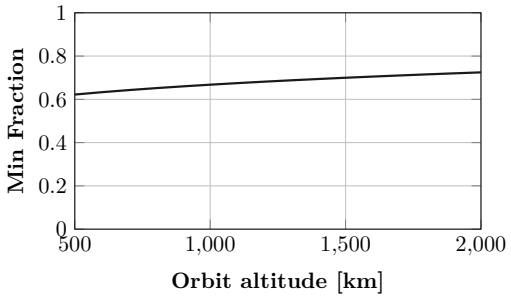

Fig. 6: Minimum fraction of orbit in sunlight

Note that these calculations are the worst case scenario for an orbit. For different inclination and Right Ascension of the Ascending Node (RAAN) angles, the fraction of an orbit in sunlight will be greater. We can see that this minimum fraction ranges from 60% to 70% for altitudes of 500km to 2000km. Also, it is worth noticing that some of the orbits might not have an eclipse at all, e.g. SSO.

Furthermore, we consider four target approach directions: from positive R-bar direction, negative R-bar, positive V-bar and negative V-bar, see Fig.7.

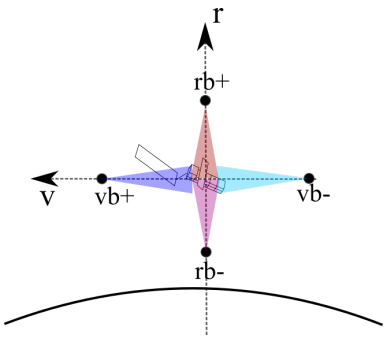

Fig. 7: Different approach directions with field-of-view of the camera depicted

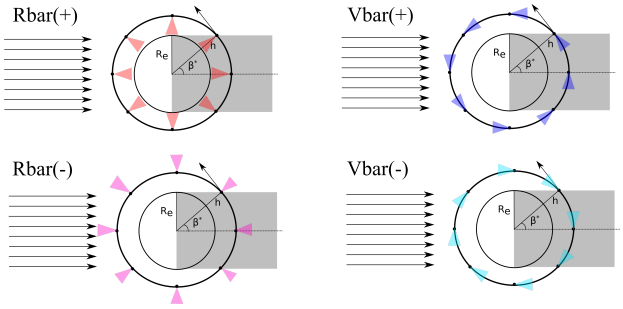

Fig. 8: Different approach directions

When combined with eclipse conditions, each of the four approach directions experiences varying illumination during the orbit, as shown in Fig. 8. All of the approach directions will cycle 360°, however, the difference is in which part of the orbit the field of view is pointing towards the sun. For the R-bar (+) approach, this happens during eclipse, and thus the useful part of the orbit is not affected. The R-bar (-) has it on the opposite side, thus the camera would be blinded by the sun in the mid-way of the illuminated part of the orbit. The two V-bar approaches are symmetrical and will experience the sun in the field of view on the two opposite legs.

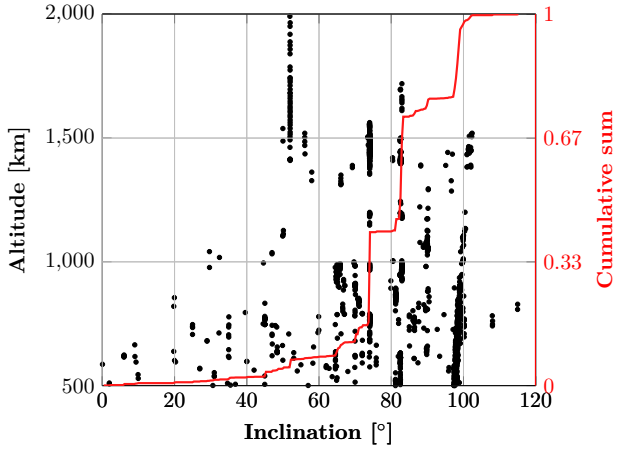

Fig. 9: Distribution of potential RSO to capture

The R-bar (+) approach is optimal in terms of illumination but suffers from the Earth's visibility in the background, which can confuse line detection algorithms and degrade pose estimation accuracy. Although some machine learning (ML) methods can easily cope with this situation, the LSD detector might detect lines that are not associated with the target, and thus the PPL algorithm would not work properly. For a black background, the R-bar (-) approach is more favorable, as it always points away from the planet. However, as mentioned before, the illuminated part of the orbit is split into two parts that will have the illumination conditions needed.

5. Orbital assessment of the debris

Next, we analyze the orbits of the debris and their respective illumination conditions. We retrieved data from the Celestrak [13] catalog, filtering for inactive objects categorized as *payloads*, *rocket bodies* and *unknown*. These are referred to as Resident Space Objects (RSOs). Furthermore, these were filtered to reside in Low Earth Orbits (LEO) with close to zero eccentricities. Of the 2104 objects left, there are 1425 inactive satellites, 646 rocket bodies, and 33 unknown objects. The distribution of these objects over inclination and average altitude is presented in Fig. 9.

The majority of the RSOs are above the 70° inclination, with a significant portion at Sun-Synchronous Orbits (SSO). In fact, the 50 statistically most concerning objects in LEO are above the 70° inclination and altitude range between 800-1000km [14]. These are mainly old Russian satellites (Cosmos) and second-stage Zenit rockets. Notably, ESA's Envisat is the only European object on this list.

The orbits of RSOs were propagated in time (for one year), including gravitational perturbations (orbital precession) and the changing direction of the sun. The four approach directions are evaluated to see what fraction of the orbit for each approach is available. The average fraction is presented in Fig. 10.

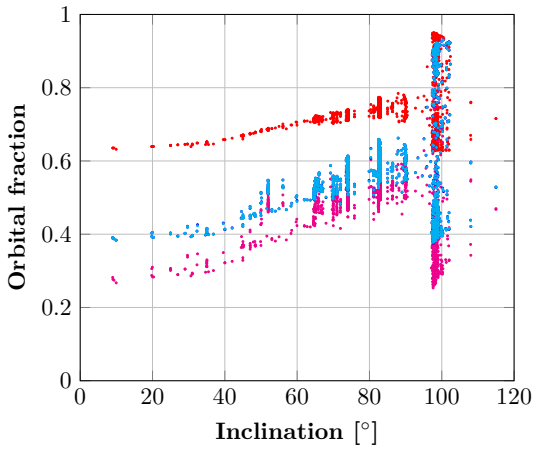

Fig. 10: Fraction of orbit with favorable conditions for PPL

In terms of sun angles, the R-bar (+) approach offers the longest part of the orbit with the required conditions, which ranges from 65% to 75%. This is true for inclinations below the SSO ones. The R-bar (-) has this fraction between 30% and 50%, while the two V-bar approaches are between 40% and 65%. For SSO orbits, this does not hold anymore, as any of the approaches might be viable, depending on the fixed sun angle at which the orbit is placed.

6. Initial pose acquisition phase in ADR missions

Some of the guidelines for an initial pose acquisition conditions are presented. Although these are specific to the PPL method, parts of the findings are generic. For other

than SSO we have:

- **Rbar(+)** approach provides the longest window of optimal illumination conditions (60-90 minutes), but has Earth in background, not suitable for PPL.
- **Rbar(-)** - has the shortest time window for required illumination conditions (30-50 min), no Earth in background .
- **Vbar(+)** and **Vbar(-)** - moderate conditions (40-60 min), a compromise between R-bar approaches. Earth's presence in the background can be managed based on the camera's field of view, allowing for flexible optimization of pose acquisition.

Finally, the object size on the focal plane is discussed. It was found that to detect the threshold of 50 lines, the object has to be ≈ 500 pixels in size. Considering a camera with 10° field of view and a 4 Mpx square sensor, for different object sizes, it will occur at different distances, see Fig. 11.

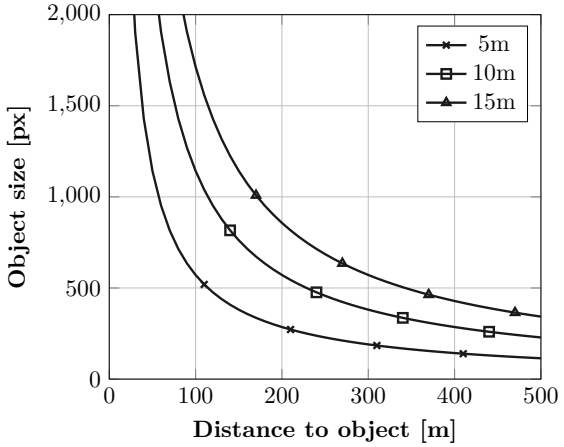

Fig. 11: Object appearance on the focal plane w.r.t. the distance for various object sizes

For objects between 5 m and 15 m, the required detection distance ranges from 100 m to 350 m, respectively. This suggests the distances where the initial acquisition phase should occur.

7. Conclusions

In this paper, we have analyzed the conditions for initial pose acquisition using the PPL method. Successful application of the PPL method requires a minimum angle of 60° between the target and the sun, a critical factor for effective pose acquisition. Different approach directions were investigated, and it was found that while the positive R-bar approach offers the best illumination conditions, its effectiveness is limited by Earth's presence in the background. Approach from the negative direction would solve the problem, but it has the least time with the right sun angle. Moreover, the illuminated part of the orbit is split into two separate sections. V-bar approaches are a compromise, depending on the field of view size, they can offer a clear background. The effect of the approach direction vanishes for high inclination and SSO orbits. Finally, the distances from which the initial pose could start to be acquired ranges from 100m - 350m, depending on the object size, which is within the safe zone of operations.

References

[1] Roberto Opromolla, Giancarmine Fasano, Giancarlo Rufino, and Michele Grassi. Pose estimation for spacecraft relative navigation using model-based algorithms. *IEEE Transactions on Aerospace and Electronic Systems*, 53(1):431–447, 2017.

[2] Alessia Nocerino, Roberto Opromolla, Giancarmine Fasano, and Michele Grassi. LIDAR-based multi-step approach for relative state and inertia parameters determination of an uncooperative target. *Acta Astronautica*, 181:662–678, April 2021.

[3] Vincenzo Capuano, Shahrouz Ryan Alimo, Andrew Q. Ho, and Soon-Jo Chung. Robust features extraction for on-board monocular-based spacecraft pose acquisition. In *AIAA Scitech 2019 Forum*.

[4] Haeyoon Han, Hanik Kim, and Hyochoong Bang. Monocular pose estimation of an uncooperative spacecraft using convexity defect features. *Sensors*, 22(21), 2022.

[5] Michele Maestrini and Pierluigi Di Lizia. Combina: Relative navigation for unknown uncooperative resident space object. In *AIAA SCITECH 2022 Forum*.

[6] Jiang Tao, Yunfeng Cao, Meng Ding, and Zhouyu Zhang. Visible and infrared image fusion-based image quality enhancement with applications to space debris on-orbit surveillance. *International Journal of Aerospace Engineering*, 2022(1):6300437, 2022.

[7] Gaia Letizia Civardi, Michele Bechini, Matteo Quirino, Alessandro Colombo, Margherita Piccinin, and Michèle Lavagna. Generation of fused visible and thermal-infrared images for uncooperative spacecraft proximity navigation. *Advances in Space Research*, 73(11):5501–5520, 2024. Recent Advances in Satellite Constellations and Formation Flying.

[8] Roberto Opromolla, Giancarmine Fasano, Giancarlo Rufino, and Michele Grassi. A review of cooperative and uncooperative spacecraft pose determination techniques for close-proximity operations. *Progress in Aerospace Sciences*, 93:53–72, 2017.

[9] Lorenzo Pasqualetto Cassinis, Robert Fonod, and Eberhard Gill. Review of the robustness and applicability of monocular pose estimation systems for relative navigation with an uncooperative spacecraft. *Progress in Aerospace Sciences*, 110:100548, 2019.

[10] Bronislovas Razgus, Michele Maestrini, and Pierluigi Di Lizia. Initial attitude acquisition for uncooperative resident space objects using principal lines. In *AIAA SCITECH 2024 Forum*.

[11] Rafael Grompone von Gioi, Jérémie Jakubowicz, Jean-Michel Morel, and Gregory Randall. Lsd: a line segment detector. *Image Processing On Line*, pages 35–55, 2012.

[12] Sagar Bhatt, Andrew Svecz, Abran Alaniz, Jiann-Woei (Jimmy) Jang, and Louis Nguyen. Thermally-constrained fuel-optimal iss maneuvers. In *AAS GNC Conference*, 02 2015.

[13] Celestrak satellite catalogue. https://celestrak.org/satcat/search.php, 2024. Accessed: 05.09.24.

[14] Darren McKnight, Rachel Witner, Francesca Letizia, Stijn Lemmens, Luciano Anselmo, Carmen Pardini, Alessandro Rossi, Chris Kunstadter, Satomi Kawamoto, Vladimir Aslanov, Juan-Carlos Dolado Perez, Vincent Ruch, Hugh Lewis, Mike Nicolls, Liu Jing, Shen Dan, Wang Dongfang, Andrey Baranov, and Dmitriy Grishko. Identifying the 50 statistically-most-concerning derelict objects in leo. *Acta Astronautica*, 181:282–291, 2021.